

Pseudodimeric complexes of 4-styrylpyridine derivatives: Structure–property relationships and a stereospecific [2 + 2]-cross-photocycloaddition in solution

Timofey P. Martyanov^{a,b}, Artem I. Vedernikov^b, Evgeny N. Ushakov^{a,b,*}, Sergey K. Sazonov^b, Nadezhda A. Aleksandrova^b, Natalia A. Lobova^b, Lyudmila G. Kuz'mina^c, Judith A.K. Howard^d, Michael V. Alfimov^b, Sergey P. Gromov^{b,e,**}

^a Institute of Problems of Chemical Physics, Russian Academy of Sciences, Chernogolovka, Moscow Region, 142432, Russian Federation

^b Photochemistry Center of RAS, FSRC "Crystallography and Photonics", Russian Academy of Sciences, Novatorov Str. 7A-1, Moscow, 119421, Russian Federation

^c N.S. Kurnakov Institute of General and Inorganic Chemistry, Russian Academy of Sciences, Leninskiy prosp. 31, Moscow, 119991, Russian Federation

^d Department of Chemistry, Durham University, South Road, Durham, DH1 3LE, United Kingdom

^e Department of Chemistry, M.V. Lomonosov Moscow State University, Leninskie Gory 1-3, Moscow, 119991, Russian Federation

ARTICLE INFO

Keywords:

Styrylpyridinium dyes
Styrylpyridines
E–*Z* photoisomerization
[2 + 2] photocycloaddition
Cyclobutanes
Crown ethers

ABSTRACT

The study addresses the spectral and photochemical properties of *N*-(3-ammoniopropyl)-4-styrylpyridinium diperchlorate and its substituted analogs containing either electron-donating (OMe, SMe, NMe₂) or electron-withdrawing (NO₂, Cl) groups on the benzene ring. These styryl dyes in MeCN form pseudodimeric complexes with uncharged 18-crown-6-containing 4-styrylpyridine due to hydrogen bonding between the ammonium group and the crown ether oxygen atoms. The stability constants of the complexes were determined by spectrophotometric and ¹H NMR titration methods. Owing to complexation, the dyes containing OMe or SMe groups and the dye with unsubstituted benzene ring undergo a stereospecific [2 + 2]-cross-photocycloaddition to the crown-containing styrylpyridine to give unsymmetrical cyclobutane derivatives as single *rctt* isomers. The structure of cyclobutanes was confirmed by X-ray diffraction analysis. The most probable conformations of the pseudodimeric complexes in MeCN were determined by density functional theory calculations. The cross-photocycloaddition quantum yields, measured upon selective excitation of the styryl dye, and other relevant data suggested that the barrier for this photoreaction increases with an increase in the reorganization energy of the singlet excited state of the dye.

1. Introduction

The wide use of [2 + 2] photocycloaddition (PCA) reaction in preparative organic photochemistry [1,2] is explained by the possibility of reducing the number of steps in the syntheses of drugs and natural products. The most common substrates for this photoreaction are cyclic α,β -unsaturated carbonyl compounds [1–3]. In the case of acyclic olefins, PCA reactions in homogeneous solutions are usually non-stereospecific and occur with low quantum yields due to competing excited state deactivation processes, such as *E*–*Z* photoisomerization. These problems can be solved with the help of various supramolecular

approaches [4,5], in particular by using molecular self-assembly owing to cation–macrocycle interactions [6–8], hydrogen bonding [9,10], metal coordination [11,12], and cation– π interactions [13,14]. For example, it has been demonstrated that non-covalent binding of two identical molecules of styryl dyes or stilbene derivatives via cation–macrocycle interactions in MeCN can provide stereoselective or even stereospecific auto-PCA, i.e. [2 + 2] photodimerization, leading to the formation of tetra(het)aryl cyclobutane derivatives [6,7]. The very high PCA quantum yields (up to 0.38) reported in the cited articles are explained by ditopic binding involving crown ether moieties. It should be emphasized that synthetic methods that provide

* Corresponding author. Institute of Problems of Chemical Physics, Russian Academy of Sciences, Chernogolovka, Moscow Region, 142432, Russian Federation.

** Corresponding author. Photochemistry Center of RAS, FSRC "Crystallography and Photonics", Russian Academy of Sciences, Novatorov str. 7A-1, Moscow, 119421, Russian Federation.

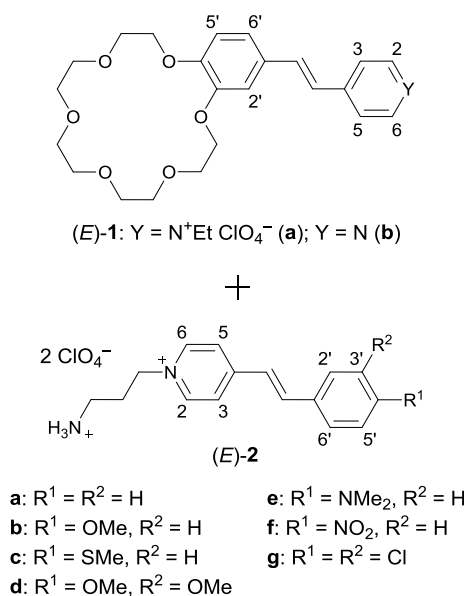
E-mail addresses: martyanov.t@gmail.com (T.P. Martyanov), artem_vedernikov@mail.ru (A.I. Vedernikov), e.n.ushakov@gmail.com (E.N. Ushakov), ssazon54@mail.ru (S.K. Sazonov), 11aha11@rambler.ru (N.A. Aleksandrova), lobova_n_a@mail.ru (N.A. Lobova), kuzmina@igic.ras.ru (L.G. Kuz'mina), j.a.k.howard@durham.ac.uk (J.A.K. Howard), alfimov@photonics.ru (M.V. Alfimov), spgromov@mail.ru (S.P. Gromov).

<https://doi.org/10.1016/j.dyepig.2019.107825>

Received 12 July 2019; Received in revised form 15 August 2019; Accepted 19 August 2019

Available online 19 August 2019

0143-7208/ © 2019 Elsevier Ltd. All rights reserved.



Scheme 1. Formation of pseudodimeric complexes (E)-1-(E)-2.

stereospecificity and high efficiency of PCA in solution are particularly valuable [15].

PCA reactions between two different olefins (cross-PCA) can significantly expand the synthetic potential. However, the efficiency of cross-PCA in supramolecular complexes of di(het)arylethylenes is difficult to predict, since fast competing processes can take place, such as photoinduced intermolecular electron transfer [16,17]. Generally, cross-PCA reactions are little understood. To the best of our knowledge, no quantitative data on the influence of substituent nature on the efficiency of cross-PCA are available from the literature.

Previously, we showed [18] that combining of olefin molecules into pairs via ditopic binding is not necessarily required for the PCA reaction to occur; complex formation through only one binding site may be sufficient (Scheme 1). Visible light irradiation of equimolar mixtures of crown-containing styryl dye (E)-1a and N-(3-ammoniopropyl)-4-styrylpyridinium dyes (E)-2a–d in MeCN led, in all cases, to the formation of *syn*-head-to-tail cross-cycloadducts. The cross-PCA reaction occurred owing to the formation of pseudodimeric complexes (E)-1a-(E)-2a–d with appropriate orientation of the components with respect to each other.

It is of interest to study the efficiency (quantum yield) of cross-PCA depending on the nature of substituents in one of the components of the pseudodimeric complex. An important condition is the possibility to selectively excite the component in which substituents vary. In the case of complexes (E)-1a-(E)-2a–d, selective excitation of dyes (E)-2a–d is impossible because of the overlap of their long-wavelength absorption bands with the absorption spectrum of dye (E)-1a. In this study, styrylpyridine (E)-1b, which does not absorb visible light, was used as the crown-containing component of pseudodimeric complexes. In a short communication [19], it was reported that the complexation of styrylpyridine (E)-1b with styryl dye (E)-2a promotes cross-PCA between

these compounds. The reaction occurred stereospecifically to give a cyclobutane derivative solely as the *rcct* isomer.

2. Experimental

2.1. Materials

Styrylpyridine (E)-1b [20,21] and dyes (E)-2a–g [18,19,22,23] were prepared by known procedures. The dyes were dried at 70 °C *in vacuo* (0.01 mmHg). Benzoic acid and Ba(ClO₄)₂ (Aldrich) were used as received. EtNH₃ClO₄ was prepared by neutralization of EtNH₂ (aq., 70%, Merck) with HClO₄ (aq., 70%, Aldrich) followed by drying at 60 °C *in vacuo*. Dyes 2 and EtNH₃ClO₄ containing perchlorate anions are non-explosive. MeCN (special purity grade, water content < 0.03%, v/v, Cryochrom) was used to prepare solutions.

2.1.1. Synthesis of complexes between compound 1b and dyes 2 (general procedure)

A mixture of compound (E)-1b (7.5 mg, 18 μmol) and dye (E)-2 (17 μmol) was dissolved in MeCN (~4 mL). If necessary, a few drops of water were added to achieve complete dissolution of the mixture. The solution was slowly (for 2–3 weeks) saturated with benzene or a mixture of benzene and dioxane (~2:1, v/v) by the vapor diffusion method at room temperature in the dark. The amorphous precipitate thus formed was decanted and dried at 80 °C *in vacuo* to give a complex between (E)-1b and (E)-2 as a yellow powder. The stoichiometry of each complex was proved by ¹H NMR in DMSO-*d*₆. In this solvent, the complexes decomposed to give a mixture of free components (ESI, Figs. S1–S6). All the resulting complexes containing perchlorate anions were non-explosive.

Complex (E)-1b-(E)-2a (hydrate) was described in lit [19].

Complex (E)-1b-(E)-2b (hydrate) was obtained in 56% yield; mp 196–199 °C. Anal. calcd for C₂₃H₂₉NO₆·C₁₇H₂₂Cl₂N₂O₉·H₂O (902.77): C, 53.22; H, 5.92; N, 4.66. Found: C, 53.09; H, 5.94; N, 4.71.

Complex (E)-1b-(E)-2c (hydrate) was obtained in 57% yield; mp 200–203 °C. Anal. calcd for C₂₃H₂₉NO₆·C₁₇H₂₂Cl₂N₂O₈S·1.5H₂O (927.84): C, 51.78; H, 5.87; N, 4.53. Found: C, 52.00; H, 5.64; N, 4.26.

Complex (E)-1b-(E)-2d_{1.5} (hydrate) was obtained in 88% yield; mp 207–211 °C. Anal. calcd for C₂₃H₂₉NO₆·1.5C₁₈H₂₄Cl₂N₂O₁₀·0.5H₂O (1173.43): C, 51.18; H, 5.67; N, 4.78. Found: C, 50.89; H, 5.54; N, 4.69.

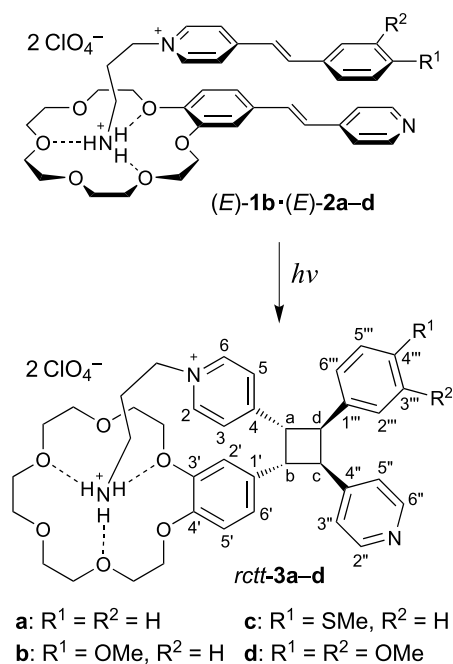
Complex (E)-1b-(E)-2f (hydrate) was obtained in 82% yield; mp 191–194 °C. Anal. calcd for C₂₃H₂₉NO₆·C₁₆H₁₉Cl₂N₃O₁₀·2H₂O (935.75): C, 50.06; H, 5.60; N, 5.99. Found: C, 50.11; H, 5.22; N, 5.91.

Complex (E)-1b-(E)-2g_{1.5} (hydrate) was obtained in 87% yield; mp 190–194 °C. Anal. calcd for C₂₃H₂₉NO₆·1.5C₁₆H₁₈Cl₄N₂O₈·0.5H₂O (1186.69): C, 47.57; H, 4.84; N, 4.72. Found: C, 47.32; H, 4.65; N, 4.55.

2.1.2. Synthesis of cyclobutanes *rcct*-3a–d (general procedure)

A mixture of compound (E)-1b (16.6 mg, 40 μmol) and dye (E)-2a–d (40 μmol) was dissolved in MeCN (15 mL) in a glass flask and irradiated with a 60 W incandescent light from a distance of ~15 cm for 120–720 h. The reaction mixture was concentrated *in vacuo* to a volume of ~5–6 mL, and this solution was slowly saturated with a mixture of benzene and dioxane (~2:1, v/v) by the vapor diffusion method at room temperature for 1–2 weeks. The crystalline precipitate thus formed was decanted and dried at 80 °C *in vacuo* to give compound *rcct*-3a–d as a slightly yellowish powder. The ¹H and ¹³C NMR spectra and the UV–Vis spectra of the resulting cyclobutane derivatives are presented in Figs. S7–S15 (ESI). The atom numbering in cyclobutanes *rcct*-3 is shown in Scheme 2. Compounds *rcct*-3 containing perchlorate anions were non-explosive.

1-(3-Ammoniopropyl)-4-*r*-[2-*c*-(2,3,5,6,8,9,11,12,14,15-decahydro-1,4,7,10,13,16-benzohexaaxacyclooctadecin-18-yl)-4-*t*-phenyl-3-*t*-4-(pyridyl)cyclobutyl]pyridinium diperchlorate (*rcct*-3a) was described in lit [19]. UV–Vis (MeCN) λ_{max} ~ 286 sh. (ε 3000), ~258 sh. (ε 7000), ~223 nm sh. (ε 21800 M⁻¹ cm⁻¹).

Scheme 2. Formation of cyclobutanes *rctt-3a-d*.

1-(3-Ammoniopropyl)-4-*r*-[2-*c*-(2,3,5,6,8,9,11,12,14,15-decahydro-1,4,7,10,13,16-benzohexaoxacyclooctadecin-18-yl)-4-*t*-(4-methoxyphenyl)-3-*t*-pyridin-4-ylcyclobutyl]pyridinium diperchlorate (*rctt-3b*) was obtained in 70% yield, mp 198–200 °C dec. UV–Vis (MeCN) λ_{\max} 284 (ϵ 4600), 230 nm (ϵ 29700 M⁻¹ cm⁻¹). ¹H NMR (500 MHz, DMSO-*d*₆, 30 °C) δ : 2.12 (m, 2H, CH₂CH₂NH₃), 2.31 (m, 1H, CHH'NH₃), 2.39 (m, 1H, CHH'NH₃), 3.63 (s, 4H, 2 CH₂O), 3.66 (m, 7H, MeO, 2 CH₂O), 3.71 (m, 4H, 2 CH₂O), 3.80 (m, 4H, 2 CH₂CH₂OAr), 3.93 (m, 2H, 3'-CH₂OAr), 4.09 (m, 2H, 4'-CH₂OAr), 4.55 (t, 2H, *J* = 6.0 Hz, CH₂N), 4.68 (m, 2H, b-CH, c-CH), 4.76 (m, 1H, d-CH), 4.83 (m, 1H, a-CH), 6.52 (d, 1H, *J* = 1.4 Hz, 2'-H), 6.76 (d, 2H, *J* = 8.7 Hz, 3''-H, 5''-H), 6.92 (d, 1H, *J* = 8.3 Hz, 5'-H), 7.05 (dd, 1H, *J* = 8.3 Hz, *J* = 1.4 Hz, 6'-H), 7.16 (d, 2H, *J* = 8.7 Hz, 2''-H, 6''-H), 7.19 (br. s, 3H, NH₃), 7.22 (d, 2H, *J* = 5.9 Hz, 3''-H, 5''-H), 7.93 (d, 2H, *J* = 6.6 Hz, 3-H, 5-H), 8.36 (d, 2H, *J* = 5.9 Hz, 2''-H, 6''-H), 8.77 (d, 2H, *J* = 6.6 Hz, 2-H, 6-H). ¹³C NMR (125 MHz, DMSO-*d*₆, 30 °C) δ : 28.10 (CH₂CH₂NH₃), 35.66 (CH₂NH₃), 42.06 (d-CH), 43.55 (c-CH), 46.68 (b-CH), 47.37 (a-CH), 54.80 (MeO), 57.13 (CH₂N), 67.04 (4'-CH₂OAr), 67.10 (3'-CH₂OAr), 68.22 (CH₂CH₂OAr), 68.42 (CH₂CH₂OAr), 68.51 (2 CH₂O), 69.09 (CH₂O), 69.18 (CH₂O), 69.56 (CH₂O), 69.67 (CH₂O), 111.57 (2'-C, 5'-C), 113.35 (3'''-C, 5'''-C), 120.35 (6'-C), 123.35 (3'-C, 5'-C), 127.20 (3-C, 5-C), 128.96 (2''-C, 6''-C), 130.53 (1'''-C), 131.17 (1'-C), 143.03 (2-C, 6-C), 145.39 (4'-C), 146.23 (3'-C), 148.86 (2''-C, 6''-C), 149.10 (4''-C), 157.64 (4'''-C), 161.21 (4-C). Anal. calcd for C₄₀H₅₁Cl₂N₃O₁₅ (884.75): C, 54.30; H, 5.81; N, 4.75; found: C, 54.44; H, 5.91; N, 4.74.

1-(3-Ammoniopropyl)-4-*r*-[2-*c*-(2,3,5,6,8,9,11,12,14,15-decahydro-1,4,7,10,13,16-benzohexaoxacyclooctadecin-18-yl)-4-*t*-[4-(methylthio)phenyl]-3-*t*-pyridin-4-ylcyclobutyl]pyridinium diperchlorate (*rctt-3c*) was obtained in 58% yield, mp 212–214 °C. UV–Vis (MeCN) λ_{\max} ~ 285 sh. (ϵ 6400), 259 (ϵ 25000), 228 nm (ϵ 27800 M⁻¹ cm⁻¹). ¹H NMR (500 MHz, DMSO-*d*₆, 30 °C) δ : 2.12 (m, 2H, CH₂CH₂NH₃), 2.32 (m, 1H, CHH'NH₃), 2.41 (m, 1H, CHH'NH₃), 2.38 (s, 3H, MeS), 3.63 (s, 4H, 2 CH₂O), 3.65 (m, 4H, 2 CH₂O), 3.71 (m, 4H, 2 CH₂O), 3.79 (m, 4H, 2 CH₂CH₂OAr), 3.93 (m, 2H, 3'-CH₂OAr), 4.08 (m, 2H, 4'-CH₂OAr), 4.55 (t, 2H, *J* = 5.9 Hz, CH₂N), 4.67 (dd, 1H, *J* = 9.6 Hz, *J* = 7.2 Hz, b-CH), 4.71 (dd, 1H, *J* = 10.0 Hz, *J* = 7.2 Hz, c-CH), 4.80 (dd, 1H, *J* = 9.6 Hz, *J* = 8.2 Hz, d-CH), 4.87 (dd, 1H, *J* = 10.0 Hz, *J* = 8.2 Hz, a-CH), 6.53 (br. s, 1H, 2'-H), 6.92 (d, 1H, *J* = 8.3 Hz, 5'-H), 7.05 (br. d, 1H, *J* = 8.3 Hz, 6'-H), 7.09 (d, 2H, *J* = 8.4 Hz, 3''-H, 5''-H), 7.18 (d, 2H,

J = 8.4 Hz, 2''-H, 6''-H), 7.20 (br. s, 3H, NH₃), 7.25 (d, 2H, *J* = 5.8 Hz, 3''-H, 5''-H), 7.94 (d, 2H, *J* = 6.5 Hz, 3-H, 5-H), 8.39 (d, 2H, *J* = 5.8 Hz, 2''-H, 6''-H), 8.78 (d, 2H, *J* = 6.5 Hz, 2-H, 6-H). ¹³C NMR (125 MHz, DMSO-*d*₆, 30 °C) δ : 14.50 (MeS), 28.08 (CH₂CH₂NH₃), 35.63 (CH₂NH₃), 42.29 (d-C), 43.59 (c-CH), 46.74 (a-CH), 46.99 (b-CH), 57.10 (CH₂N), 67.07 (3'-CH₂OAr), 67.12 (4'-CH₂OAr), 68.21 (CH₂CH₂OAr), 68.40 (CH₂CH₂OAr), 68.53 (2 CH₂O), 69.10 (CH₂O), 69.18 (CH₂O), 69.55 (CH₂O), 69.65 (CH₂O), 111.61 (5'-C), 111.69 (2'-C), 120.32 (6'-C), 123.38 (3''-C, 5''-C), 125.51 (3'''-C, 5'''-C), 127.17 (3-C, 5-C), 128.42 (2''-C, 6''-C), 131.03 (1'-C), 135.26 (1'''-C), 135.96 (4''-C), 143.04 (2-C, 6-C), 145.46 (4'-C), 146.29 (3'-C), 148.64 (2''-C, 6''-C), 149.33 (4''-C), 161.00 (4-C). Anal. calcd for C₄₀H₅₁Cl₂N₃O₁₄S (900.82): C, 53.33; H, 5.71; N, 4.67; found: C, 53.35; H, 5.74; N, 4.61.

1-(3-Ammoniopropyl)-4-*r*-[2-*c*-(2,3,5,6,8,9,11,12,14,15-decahydro-1,4,7,10,13,16-benzohexaoxacyclooctadecin-18-yl)-4-*t*-(3,4-dimethoxyphenyl)-3-*t*-pyridin-4-ylcyclobutyl]pyridinium diperchlorate (*rctt-3d*) was obtained in 33% yield, mp > 236 °C dec. UV–Vis (MeCN) λ_{\max} 282 (ϵ 6600), ~230 sh. (ϵ 30200 M⁻¹ cm⁻¹). ¹H NMR (500 MHz, DMSO-*d*₆, 30 °C) δ : 2.13 (m, 2H, CH₂CH₂NH₃), 2.35 (m, 1H, CHH'NH₃), 2.45 (m, 1H, CHH'NH₃), 3.63 (s, 4H, 2 CH₂O), 3.64 (s, 3H, 4''-OMe), 3.65 (m, 7H, 3'''-OMe, 2 CH₂O), 3.71 (m, 4H, 2 CH₂O), 3.79 (m, 4H, 2 CH₂CH₂OAr), 3.94 (m, 2H, 3'-CH₂OAr), 4.08 (m, 2H, 4'-CH₂OAr), 4.58 (t, 2H, *J* = 5.9 Hz, CH₂N), 4.70 (dd, 1H, *J* = 9.9 Hz, *J* = 6.3 Hz, b-CH), 4.74 (dd, 1H, *J* = 9.7 Hz, *J* = 6.3 Hz, c-CH), 4.79 (dd, 1H, *J* = 9.7 Hz, *J* = 7.6 Hz, d-CH), 4.89 (dd, 1H, *J* = 9.9 Hz, *J* = 7.6 Hz, a-CH), 6.57 (d, 1H, *J* = 1.2 Hz, 2'-H), 6.74–6.79 (m, 3H, 2''-H, 5''-H, 6''-H), 6.91 (d, 1H, *J* = 8.4 Hz, 5'-H), 7.04 (dd, 1H, *J* = 8.4 Hz, *J* = 1.2 Hz, 6'-H), 7.27 (br. s, 3H, NH₃), 7.41 (d, 2H, *J* = 5.4 Hz, 3''-H, 5''-H), 7.96 (d, 2H, *J* = 6.6 Hz, 3-H, 5-H), 8.46 (d, 2H, *J* = 5.4 Hz, 2''-H, 6''-H), 8.83 (d, 2H, *J* = 6.6 Hz, 2-H, 6-H). ¹³C NMR (125 MHz, DMSO-*d*₆, 30 °C) δ : 28.09 (CH₂CH₂NH₃), 35.60 (CH₂NH₃), 42.78 (d-CH), 44.04 (c-CH), 46.32 (b-CH), 47.02 (a-CH), 55.26 (3'''-OMe), 55.40 (4''-OMe), 57.01 (CH₂N), 67.10 (4'-CH₂OAr), 67.24 (3'-CH₂OAr), 68.24 (CH₂CH₂OAr), 68.41 (CH₂CH₂OAr), 68.56 (2 CH₂O), 69.13 (CH₂O), 69.20 (CH₂O), 69.55 (CH₂O), 69.67 (CH₂O), 111.24 (5'''-C), 111.63 (5'-C), 111.87 (2'-C), 112.28 (2''-C), 119.80 (6''-C), 120.29 (6'-C), 123.96 (3''-C, 5''-C), 127.16 (3-C, 5-C), 130.81 (1'''-C), 131.03 (1'-C), 143.05 (2-C, 6-C), 145.53 (4'-C), 146.36 (3'-C), 147.20 (2''-C, 6''-C, 3''-C), 147.36 (4''-C), 148.18 (4''-C), 161.09 (4-C). Anal. calcd for C₄₁H₅₃Cl₂N₃O₁₆ (914.78): C, 53.83; H, 5.84; N, 4.59; found: C, 53.76; H, 5.96; N, 4.44.

2.2. Methods

Melting points were measured on a Mel-Temp II instrument. ¹H and ¹³C NMR spectra were recorded on a Bruker DRX500 instrument in DMSO-*d*₆ using the solvent as the internal reference (δ_{H} 2.50 and δ_{C} 39.43). 2D NOESY spectra and ¹H–¹³C correlation spectra (HSQC and HMBC) were used to assign the proton and carbon signals; the mixing time in the NOESY experiments was 300 μ s. Elemental analysis was carried out at the Microanalytical Laboratory of the A.N. Nesmeyanov Institute of Organoelement Compounds (Russian Academy of Sciences, Moscow). The samples for elemental analysis were dried at 80 °C *in vacuo*. Electronic absorption spectra were recorded on a Specord M40 spectrophotometer in quartz cells with ground-in stoppers. All manipulations with solutions of compound **1b** and dyes **2** were performed in a darkroom under red light (daylight induces the *E*–*Z* photoisomerization). Stationary photolysis was performed using glass-filtered light of a high pressure Hg lamp (λ = 313, 365, 405, or 436 nm); the light intensity was measured by chemical actinometry. Fluorescence spectra were recorded on a PerkinElmer LS 55 spectrometer at a constant photodetector voltage and corrected using the spectral sensitivity curve for the photodetector, as provided by the supplier. Fluorescence lifetimes were measured on a PicoQuant FluoTime 200 spectrometer using a semiconductor pulsed laser as the excitation source (λ = 375 nm, pulse duration ~75 ps).

2.3. Fluorescence quantum yields and lifetimes

Fluorescence quantum yields (ϕ_{fl}) were determined using anthracene in ethanol as the reference. The value of ϕ_{fl} was calculated by the formula

$$\phi_{\text{fl}} = (\phi_{\text{fl},r} D_{\text{ex},r} n^2 S) / (D_{\text{ex}} n_r^2 S_r)$$

where the subscript r refers to the parameters of the reference, D_{ex} is the optical density at the excitation wavelength, n is the refractive index of the solvent, S is the integrated intensity of the corrected fluorescence spectrum in the energy scale, $\phi_{\text{fl},r} = 0.28$ [24].

Fluorescence lifetimes were determined by global analysis of the fluorescence decay curves measured at three different wavelengths. The general procedure for the global analysis of pulse spectroscopy data has been described previously [16].

2.4. E-Z photoisomerization quantum yields

The quantum yields for the forward and back E-Z photoisomerization reactions ($\phi_{E \rightarrow Z}$ and $\phi_{Z \rightarrow E}$) were determined from the kinetics of absorption spectra observed upon steady-state irradiation of a solution of E-isomer with 365 nm light. The absorption spectrum of the pure Z-isomer was calculated using the spectra of the E-Z photostationary states attained upon irradiation at different wavelengths on the assumption that the $\phi_{E \rightarrow Z} / \phi_{Z \rightarrow E}$ ratio is independent of the irradiation wavelength. The spectroscopic data were treated using global analysis methods, as described previously [22]. The photoisomerization quantum yields are measured to within $\pm 20\%$.

2.5. Spectrophotometric titration (SPT)

SPT experiments were conducted in MeCN in 1 cm cells. In the (E)-1b-(E)-2 systems, the total concentration of dye (E)-2 was maintained constant, and the total concentration of ligand (E)-1b increased incrementally starting from zero. The experiments with the (E)-1b-EtNH₃ClO₄ system were carried out at a fixed total concentration of the ligand. The stability constants and the absorption spectra of pure complexes (E)-1b-(E)-2 and (E)-1b-EtNH₃⁺ were determined by globally fitting the SPT data to a 1:1 complexation model.

2.6. Cross-PCA quantum yields

Equimolar solutions of compound (E)-1b with dyes (E)-2b-d [MeCN, (1–2) × 10⁻⁴ M, 0.2 cm cell] were irradiated with 436 nm light (selective excitation of the dye). The dye consumption in the cross-PCA reaction was determined by spectrophotometry using the nonstandard procedure described previously [22]. The measured cross-PCA quantum yields are effective values, because the dyes complexed with (E)-1b underwent also the reversible E-Z photoisomerization.

2.7. ¹H NMR titration

Experiments were conducted in MeCN-d₃-D₂O solutions (98:2, v/v). MeCN-d₃ was used as the internal reference (δ_{H} 1.96). The stability constants of the complexes of ligand (E)-1b with dyes (E)-2a-g were determined by analyzing the shifts of the proton signals of the ligand ($\Delta\delta_{\text{H}}$) as a function of the concentration of the added dye. The total ligand concentration was maintained constant ($\sim 1 \times 10^{-3}$ M), and the total dye concentration varied from 0 to $\sim 3 \times 10^{-3}$ M. The $\Delta\delta_{\text{H}}$ values were measured to an accuracy of 0.001 ppm. In all cases, the titration data were well fit to a 1:1 complexation model. The calculations were performed using the HYPNMR program [25].

2.8. X-ray diffraction experiments

The crystals of structure (E)-1b-PhCO₂H were grown from a MeCN-benzene solution ($\sim 1:1$, v/v) of equimolar mixture of the components, which was slowly saturated with a benzene-hexane mixture ($\sim 1:2$, v/v) by the vapor diffusion method at ambient temperature in the dark. The crystals of cyclobutanes *rctt*-3b-d were obtained by slow saturation of their acetonitrile solutions with benzene by the vapor diffusion method at ambient temperature.

The single crystals of all compounds were coated with perfluorinated oil and mounted on a Bruker SMART-CCD diffractometer [graphite monochromatized Mo-K α radiation ($\lambda = 0.71073$ Å), ω scan mode] under a stream of cold nitrogen [$T = 180(2)$ K for *rctt*-3b-C₆H₆ or 120(2) K for other structures]. The sets of experimental reflections were measured, and the structures were solved by direct methods and refined with anisotropic thermal parameters for all non-hydrogen atoms (except for some oxygen atoms of the disordered perchlorate anions in the cyclobutane structures which were refined isotropically). The hydrogen atoms were fixed at calculated positions at carbon and nitrogen atoms and then refined with an isotropic approximation for (E)-1b-PhCO₂H or by using a riding model for other structures. The hydrogen atom of the CO₂H group in structure (E)-1b-PhCO₂H was found from the Fourier syntheses and then refined isotropically. In structure *rctt*-3c-2C₆H₆·H₂O, the hydrogen atoms of the water molecule of solvation were not located.

Crystal data for (E)-1b-PhCO₂H: C₃₀H₃₅NO₈, $M = 537.59$, monoclinic, space group *Pc* (no. 7), colorless block, $a = 17.2080(6)$ Å, $b = 9.5488(3)$ Å, $c = 8.4774(3)$ Å, $\beta = 101.569(3)^\circ$, $V = 1364.67(8)$ Å³, $T = 120(2)$ K, $Z = 2$, $\mu = 0.095$ mm⁻¹, $\rho_{\text{calc}} = 1.308$ g cm⁻³, $2\theta_{\text{max}} = 58.00^\circ$, 13601 reflections measured, 6719 unique ($R_{\text{int}} = 0.0393$), $R_1 = 0.0439$ (5685 reflections with $I > 2\sigma(I)$), $wR_2 = 0.0828$ (all data), goodness-on-fit on $F^2 = 1.005$, 492 parameters, min/max residual electron density = $-0.245/0.258$ e Å⁻³. No constraints were applied.

Crystal data for *rctt*-3b-C₆H₆: C₄₆H₅₇Cl₂N₃O₁₅, $M = 962.84$, monoclinic, space group *P2₁/n* (no. 14), colorless block, $a = 12.7862(18)$ Å, $b = 26.667(4)$ Å, $c = 13.7651(19)$ Å, $\beta = 98.267(2)^\circ$, $V = 4644.7(11)$ Å³, $T = 180(2)$ K, $Z = 4$, $\mu = 0.212$ mm⁻¹, $\rho_{\text{calc}} = 1.377$ g cm⁻³, $2\theta_{\text{max}} = 54.00^\circ$, 33796 reflections measured, 10103 unique ($R_{\text{int}} = 0.0514$), $R_1 = 0.0803$ (5766 reflections with $I > 2\sigma(I)$), $wR_2 = 0.2532$ (all data), goodness-on-fit on $F^2 = 1.107$, 674 parameters, min/max residual electron density = $-0.772/0.698$ e Å⁻³. Perchlorate anions Cl(1)O₄ and Cl(2)O₄ are disordered both over three positions with the occupancy ratios of 0.70:0.15:0.15 and 0.60:0.20:0.20. Two independent benzene molecules of solvation are situated at the symmetry centers of the unit cell. These two benzene molecules are disordered both over two positions with the occupancy ratios of 0.73:0.27 and 0.63:0.37. SADI and ISOR commands were applied for the atoms of the strongly disordered moieties in order to constrain their geometry and anisotropic thermal parameters.

Crystal data for *rctt*-3c-2C₆H₆·H₂O: C₅₂H₆₅Cl₂N₃O₁₅S, $M = 1075.03$, triclinic, space group *p* $\bar{1}$ (no. 2), colorless plate, $a = 11.866(4)$ Å, $b = 12.966(4)$ Å, $c = 17.585(6)$ Å, $\alpha = 96.265(15)^\circ$, $\beta = 98.848(16)^\circ$, $\gamma = 99.858(17)^\circ$, $V = 2608.4(15)$ Å³, $T = 120(2)$ K, $Z = 2$, $\mu = 0.236$ mm⁻¹, $\rho_{\text{calc}} = 1.369$ g cm⁻³, $2\theta_{\text{max}} = 50.00^\circ$, 11624 reflections measured, 7889 unique ($R_{\text{int}} = 0.2669$), $R_1 = 0.1160$ (1841 reflections with $I > 2\sigma(I)$), $wR_2 = 0.2884$ (all data), goodness-on-fit on $F^2 = 0.761$, 658 parameters, min/max residual electron density = $-0.490/0.520$ e Å⁻³. The very thin-plate shape of the crystal resulted in a decrease in the accuracy of this X-ray diffraction experiment. Perchlorate anion Cl(1)O₄ is disordered over two positions with the occupancy ratio of 0.60:0.40. SADI command was applied for the atoms of this anion in order to constrain its geometry. ISOR command was applied for some atoms to constrain their anisotropic thermal parameters.

Crystal data for *rctt*-3d-1.5C₆H₆: C₅₀H₆₂Cl₂N₃O₁₆, $M = 1031.92$,

triclinic, space group $P\bar{1}$ (no. 2), colorless block, $a = 11.2596(16)$ Å, $b = 14.300(2)$ Å, $c = 16.256(2)$ Å, $\alpha = 79.466(5)^\circ$, $\beta = 83.912(6)^\circ$, $\gamma = 88.356(6)^\circ$, $V = 2558.6(6)$ Å³, $T = 120(2)$ K, $Z = 2$, $\mu = 0.199$ mm⁻¹, $\rho_{\text{calc}} = 1.339$ g cm⁻³, $2\theta_{\text{max}} = 54.00^\circ$, 18388 reflections measured, 11018 unique ($R_{\text{int}} = 0.1021$), $R_1 = 0.1108$ (4283 reflections with $I > 2\sigma(I)$), $wR_2 = 0.3088$ (all data), goodness-on-fit on $F^2 = 0.902$, 672 parameters, min/max residual electron density = $-0.374/0.810$ e Å⁻³. Perchlorate anion Cl(2)O₄ is disordered over four close positions with the occupancy ratio of 0.25:0.25:0.25:0.25. SADI command was applied for the atoms of this anion in order to constrain its geometry. One of the two independent benzene molecules of solvation is situated at the symmetry centre of the unit cell. SADI and ISOR commands were applied for the carbon atoms of this benzene molecule to constrain its geometry and anisotropic thermal parameters of the atoms.

All the calculations were performed using the SHELXL software [26]. The crystallographic data for (E)-1b-PhCO₂H, rctt-3b-C₆H₆, rctt-3c-2C₆H₆·H₂O, and rctt-3d-1.5C₆H₆ have been deposited with the Cambridge Crystallographic Data Centre under numbers CCDC 1918671, 1918672, 1918673, and 1918674, respectively.

2.9. Density functional theory (DFT) calculations

DFT calculations were performed using the Gaussian 16 program package [27]. Geometry optimizations were carried out with the M06-2X functional [28] and the 6-31G(d) basis set. To accelerate calculations, the two-electron integral accuracy was set to 10^{-10} (the default value is 10^{-12}). The default optimization criteria were tightened by three times using the internal option IOp(1/7 = 100). The SMD polarizable continuum model [29] was employed to simulate effects of MeCN as the experimental solvent. To specify a finer surface discretization in the SMD calculations, the average density of integration points on the surface was set to 15 Å⁻² for free styryl dyes and to 10 Å⁻² in all other cases (the default value is 5 Å⁻²). All geometry optimizations were followed by frequency calculations to verify the nature of stationary points and to compute thermochemical quantities. The thermochemical analysis was carried out using a scale factor of 0.96 for harmonic frequencies. The Gibbs free energy in solution (G_{soln}) was calculated by the formula

$$G_{\text{soln}} = E_{\text{soln}} + \Delta G_{\text{corr}}$$

where E_{soln} is the electronic energy in solution, and ΔG_{corr} is the thermal correction to the free energy, including the zero-point vibrational energy. The ΔG_{corr} values were calculated at the same level of theory as that used for geometry optimizations, whereas the E_{soln} values were derived from the single-point M06-2X calculations with the 6-311G(2df, 2p) basis set.

3. Results and discussion

3.1. Photochemical study

Fig. 1 shows the absorption and fluorescence spectra of styryl dye (E)-2b in MeCN, as well as spectrophotometric data on the steady-state photolysis of this compound. The corresponding data for (E)-1b, (E)-2a, and (E)-2c-e are presented in Figs. S16 and S17 (ESI). Crown-compound (E)-1b and dyes (E)-2a-e demonstrate an intense S₀-S₁ absorption band associated with the π - π^* transition. All these compounds except (E)-2e undergo photochemically reversible E-Z photoisomerization, resulting in spectral changes typical of 1,2-di(het)arylethenes. Dye (E)-2e containing a dimethylamino group is not only photoinert, but also almost non-fluorescent in MeCN. Presumably, these properties are related to rapid conversion of the initial excited state to the twisted internal charge-transfer (TICT) state [30,31], followed by nonradiative deactivation.

The key spectroscopic and photochemical characteristics of

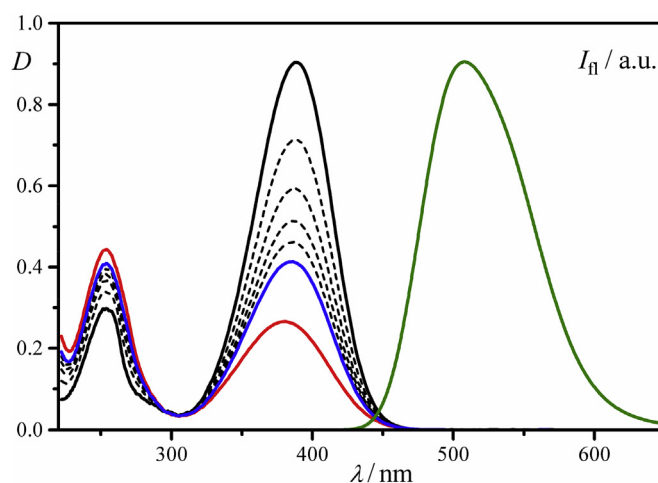


Fig. 1. Spectrophotometric data on the steady-state photolysis of dye (E)-2b with 365 nm light: MeCN, 1 cm cell, total dye concentration 2.44×10^{-5} M, light intensity 2.8×10^{-9} mol cm⁻² s⁻¹. The solid black curve is the spectrum of (E)-2b; the blue curve is the spectrum of the E-Z photostationary state; the red curve is the spectrum of (Z)-2b; the dashed curves are recorded after irradiation for 8.5, 16.3, 24.2, and 34.1 s; the green curve is the corrected fluorescence spectrum of (E)-2b (4.6×10^{-6} M, excitation at 347 nm). (For interpretation of the references to color in this figure legend, the reader is referred to the Web version of this article.)

compounds (E)-1b and (E)-2a-e are presented in Table 1. The S₀-S₁ transition of styryl dyes (E)-2a-e involves charge transfer between the aryl moiety and the pyridinium ring; therefore, the introduction of electron-donating groups into the benzene ring of (E)-2a induces bathochromic changes in the absorption and fluorescence spectra, as well as an increase in the Stokes shift.

Analysis of the fluorescence quantum yields (ϕ_f), the emission lifetimes (τ_f), and the E-Z photoisomerization quantum yields (ϕ_{E-Z}) measured for (E)-1b and (E)-2a-c leads to the conclusion that the main channel of the singlet excited state deactivation for these compounds is E-Z photoisomerization, although for the dye containing the SMe group, radiative transition makes a comparable contribution to deactivation. Judging by the available data, the barrier for E-Z photoisomerization and the fluorescence lifetime increase in series (E)-2a-c (τ_f increases more than tenfold). The Stokes shift and, hence, the reorganization energy of the singlet excited state increases in the same series. That is, the following correlation holds: the barrier for E-Z photoisomerization grows with increasing reorganization energy.

Specific features of dye (E)-2d, which has two OMe groups on the benzene ring, are biexponential fluorescence decay and relatively small sum of ϕ_f and ϕ_{E-Z} (about 0.11) as compared with dyes (E)-2a-c. The slower decay component ($\tau_f = 0.48$ ns) makes the major contribution to the overall fluorescence yield (see caption to Fig. S18, ESI). The small sum of ϕ_f and ϕ_{E-Z} indicates another pathway for nonradiative deactivation of the excited state, faster than the E-Z photoisomerization. The reasons for the unusual excited-state behavior of dye (E)-2d are obscure.

Table 2 shows the stability constants of the complexes formed by crown-compound (E)-1b with the EtNH₃⁺ ion and dyes (E)-2b-e in MeCN, as measured by spectrophotometric titration (SPT). The main spectroscopic and photochemical characteristics of complexes (E)-1b-(E)-2b-e are presented in the same table. The SPT data for systems (E)-1b-EtNH₃⁺ and (E)-1b-(E)-2b are shown in Fig. 2.

The complexation of (E)-1b with EtNH₃⁺ induces a blue shift of the absorption band of the crown compound (by 7 nm, Fig. 2a). The cation-induced hypsochromic effects are typical of related donor-acceptor chromoionophores based on crown ethers [32,33]. The formation of pseudodimeric complexes (E)-1b-(E)-2b-e is accompanied by a slight

Table 1
Spectroscopic and photochemical characteristics of compounds (*E*)-**1b** and (*E*)-**2a–e**.^a

Compound	$\lambda_{\max}^{\text{abs}}$, nm	$\epsilon_{\max} \times 10^{-4}$, M ⁻¹ cm ⁻¹	$\lambda_{\max}^{\text{fl}}$, nm	E_{SS} , cm ⁻¹	ϕ_{fl}	τ_{fl} , ns	ϕ_{E-Z}	ϕ_{Z-E}
(<i>E</i>)- 1b	333	2.58	422	6330	0.097	–	0.44	0.32
(<i>E</i>)- 2a	350	3.36	433	5480	0.0014	< 0.1	0.54	0.37
(<i>E</i>)- 2b	389	3.73	508	6020	0.014	< 0.1	0.46	0.41
(<i>E</i>)- 2c	401	3.72	571	7420	0.26	1.3	0.27	0.42
(<i>E</i>)- 2d	404	3.54	563	6990	0.053	0.13, 0.48	0.055	0.51
(<i>E</i>)- 2e	483	4.17	–	–	< 10 ⁻⁴	< 0.1	–	–

^a In MeCN, $\lambda_{\max}^{\text{abs}}$ is the position of the S₀–S₁ absorption band maximum, ϵ_{\max} is the molar absorptivity at $\lambda_{\max}^{\text{abs}}$, $\lambda_{\max}^{\text{fl}}$ is the position of the fluorescence maximum in the corrected spectrum, E_{SS} is the Stokes shift, ϕ_{fl} is the fluorescence quantum yield, τ_{fl} is the fluorescence lifetime, ϕ_{E-Z} and ϕ_{Z-E} are the quantum yields of the reversible *E*–*Z* photoisomerization.

red shift and insignificant decrease in the intensity of the absorption band of the styryl dye (Fig. 2b and Table 2). Previously, we observed a similar, but more pronounced effect when studying the ditopic binding of a bis-ammonium analog of dye (*E*)-**2c** to bis(18-crown-6)stilbene [17]. This effect was attributed to stacking interactions between the complexed molecules. The formation of complexes (*E*)-**1b**(*E*)-**2b–e** also induces minor blue shift of the fluorescence spectrum of the dye; simultaneously, the fluorescence quantum yield is approximately halved (cf. data in Tables 1 and 2).

The stability constants K (M⁻¹) of complexes (*E*)-**1b**(*E*)-**2b–e** are 2–3 times higher than that of complex (*E*)-**1b**EtNH₃⁺. This is attributable to the stabilizing effect of stacking interactions in pseudodimeric complexes and, perhaps, to a somewhat greater charge of the ammonium group in the dyes as compared with EtNH₃⁺. In the series of complexes (*E*)-**1b**(*E*)-**2b–e**, the stability constant tends to slightly decrease with increasing electron-donating strength of the substituents on the benzene ring of the styryl dye, but the large measurement error of K ($\pm 30\%$) does not allow us to draw a reliable conclusion about this tendency.

Prolonged irradiation of equimolar solutions of (*E*)-**1b** and (*E*)-**2a–d** with visible light resulted, in each case, in almost complete conversion of both compounds to the cross-cycloadduct (*rctt*)-**3a–d**, Scheme 2), which does not absorb visible light (ESI, Fig. S15). The structure of cyclobutanes *rctt*-**3a–d** was determined by NMR spectroscopy and X-ray diffraction analysis (Sections 3.2 and 3.3).

The cross-PCA quantum yields (Φ_{PCA}) for complexes (*E*)-**1b**(*E*)-**2b–d**, as measured upon selective excitation of the styryl dye, are presented in Table 2. The Φ_{PCA} value decreases approximately by half in series **2b** > **2d** > **2c** (Table 2), whereas the lifetime of the singlet excited state of the dye increases more than tenfold (Table 1). This means that the rate constant of the cross-PCA reaction (k_{PCA}) dramatically decreases in this series of dyes. The molecular structure calculations presented in Section 3.4 predict that complexes (*E*)-**1b**(*E*)-**2b** and (*E*)-**1b**(*E*)-**2c** are very similar both in the geometric characteristics and in the conformational distribution. That is, these factors cannot be responsible for the contrasting difference in k_{PCA} between these two complexes. While analyzing the data presented in Tables 1 and 2, one can note that k_{PCA} decreases with increasing Stokes shift (E_{SS}) of the dye and, hence, with increasing reorganization energy of the singlet excited

Table 2
Stability constants and the spectroscopic and photochemical characteristics of the complexes of crown-compound (*E*)-**1b** with the EtNH₃⁺ ion and dyes (*E*)-**2b–e**.^a

Complex	log K	$\lambda_{\max}^{\text{abs}}$, nm	$\Delta\lambda^{\text{abs}}$, nm	$\epsilon_{\max} \times 10^{-4}$, M ⁻¹ cm ⁻¹	$\lambda_{\max}^{\text{fl}}$, nm	E_{SS} , cm ⁻¹	ϕ_{fl}	$\Phi_{\text{PCA}} \times 10^3$
(<i>E</i>)- 1b EtNH ₃ ⁺	4.03	326	–7	2.70	–	–	–	–
(<i>E</i>)- 1b (<i>E</i>)- 2b	4.58	392	+3	3.62	502	5590	0.006	3.0
(<i>E</i>)- 1b (<i>E</i>)- 2c	4.48	402	+1	3.67	566	7210	0.10	1.4
(<i>E</i>)- 1b (<i>E</i>)- 2d	4.38	406	+2	3.53	562	6840	0.03	2.6
(<i>E</i>)- 1b (<i>E</i>)- 2e	4.27	485	+2	3.87	–	–	< 10 ⁻⁴	< 0.1

^a In MeCN, the K values (M⁻¹) are measured to within about $\pm 30\%$, $\Delta\lambda^{\text{abs}}$ is the complexation induced shift of $\lambda_{\max}^{\text{abs}}$, Φ_{PCA} is the effective value of the cross-PCA quantum yield (selective excitation of the styryl dye with 436 nm light).

state (half of the E_{SS} value approximately corresponds to the reorganization energy [34]). It is known that the crucial effect on the rate constant of PCA is made by topochemical factors [35,36]. We assume that the excited state reorganization energy is also important.

Complex (*E*)-**1b**(*E*)-**2e** proved to be photoinert upon irradiation with visible light. Like in the case of free dye (*E*)-**2e**, the photoinert behavior is, most likely, due to fast nonradiative deactivation of the excited state of the dye via the TICT state.

3.2. NMR spectroscopy study

The formation of pseudodimeric complexes of styrylpyridine (*E*)-**1b** with dyes (*E*)-**2a–g** is evident from comparison of the ¹H NMR spectra of individual compounds and their equimolar mixtures. For example, the signals from ethylene protons and most aromatic protons of (*E*)-**1b** and (*E*)-**2b** in a MeCN-*d*₃-D₂O solution (98:2, v/v) shift upfield ($\Delta\delta_{\text{H}}$ up to –0.27 ppm) upon equimolar mixing of these compounds (Fig. 3, the proton numbering is shown in Scheme 1). Conversely, the signals of the CH₂O groups of the crown ether moiety of (*E*)-**1b** move downfield ($\Delta\delta_{\text{H}}$ up to 0.10 ppm, Fig. 4), which confirms hydrogen bonding of the ammonium group to the crown ether [37]. The signals of the (CH₂)₃NH₃⁺ group of the styryl dye shift upfield ($\Delta\delta_{\text{H}}$ up to –0.25 ppm).

The upfield shifts observed upon equimolar mixing of (*E*)-**1b** and (*E*)-**2b** indicate that the styrylpyridine and styrylpyridinium moieties in complex (*E*)-**1b**(*E*)-**2b** are located approximately one above the other (Scheme 1), which gives rise to various anisotropic effects. Note that the signal of the methoxy group of dye (*E*)-**2b** virtually does not shift in the presence of (*E*)-**1b**. This is due to the remoteness of this group from the ammonium ion bound to the crown ether. Similar changes in proton chemical shifts were observed upon equimolar mixing of (*E*)-**1b** with (*E*)-**2c–g** (ESI, Figs. S20–S29) and, previously, upon the formation of complexes (*E*)-**1b**(*E*)-**2a** [19] and (*E*)-**1a**(*E*)-**2a–g** [18,22,23].

The stability constants of the complexes of crown-compound (*E*)-**1b** with dyes (*E*)-**2a–g**, measured by ¹H NMR titration in a MeCN-*d*₃-D₂O solution (98:2, v/v), are summarized in Table 3. The solubilities of the dyes in anhydrous MeCN-*d*₃ were too low to attain the required concentration ($\sim 6 \times 10^{-3}$ M). The addition of a small amount of water to the solvent significantly increased the solubility.

Comparison of the data given in Tables 2 and 3 shows that the

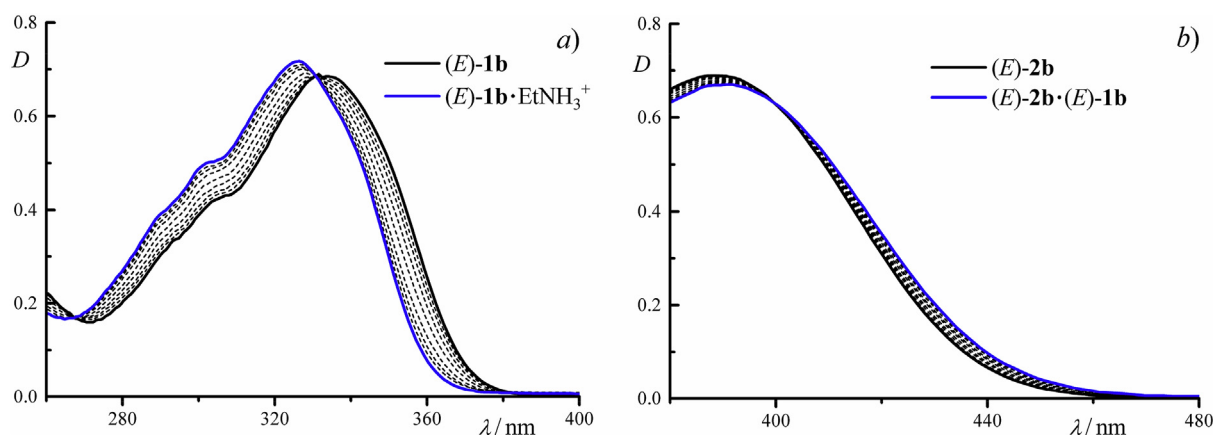


Fig. 2. Spectrophotometric titration data for the systems (a) $(E)\text{-1b}\text{-EtNH}_3^+$ and (b) $(E)\text{-1b}\text{-}(E)\text{-2b}$ in MeCN (1 cm cell): (a) 2.5×10^{-5} M $(E)\text{-1b}$, the concentration of EtNH_3^+ varies from 0 to 1×10^{-3} M; (b) 1.9×10^{-5} M $(E)\text{-2b}$, the concentration of $(E)\text{-1b}$ varies from 0 to 2.3×10^{-4} M.

presence of 2% water in the solvent decreases the stability constants of complexes $(E)\text{-1b}\text{-}(E)\text{-2b-e}$ by almost an order of magnitude, which is due to relatively high hydration energy of ammonium ions. The $\log K$ values measured in the water-containing solvent vary in the narrow range of 3.5–3.9; the maximum deviation from the mean value is only slightly higher than the measurement error.

The pseudodimeric complexes were obtained in the solid state by slow crystallization of equimolar mixtures of the components (see Section 2.1.1). Most of the complexes have 1:1 stoichiometry (according to ^1H NMR data and elemental analysis). An exception is provided by complexes of $(E)\text{-1b}$ with dyes $(E)\text{-2d,g}$, which were found to have 1:1.5 stoichiometry (this result was reproduced in several crystallizations). Apparently, the fine-crystalline phase formed in these cases was composed of the 1:1 complex co-crystallized with the free dye. Previously we observed the same stoichiometry for co-crystallized dyes $(E)\text{-1a}$ and $(E)\text{-2d}$ [18].

According to the data presented in Section 3.1, cross-PCA is relatively efficient for complexes $(E)\text{-1b}\text{-}(E)\text{-2b-d}$. This allowed us to obtain cyclobutane derivatives **3b-d** in preparative amounts by prolonged visible light irradiation of equimolar solutions of $(E)\text{-1b}$ and $(E)\text{-2b-d}$

(see Section 2.1.2). The ^1H NMR spectra of the photoproducts exhibit a set of signals in the 4.6–5.0 ppm region (ESI, Figs. S8–S10), which is characteristic of cyclobutane derivatives with a structure similar to **3b-d** [18,19]. Comparison of these signals with analogous signals of the previously studied compound *rctt-3a* (ESI, Fig. S7) suggests that cyclobutanes **3b-d**, like **3a**, have *rctt* stereochemistry and, hence, they are formed from pseudodimeric complexes $(E)\text{-1b}\text{-}(E)\text{-2b-d}$ with the *syn*-head-to-tail orientation of the styrylpyridine and styrylpyridinium moieties with respect to each other (Scheme 2). In the case of *rctt-3a,c,d*, the signals of the cyclobutane ring protons only slightly overlap with one another to manifest as four doublets of doublets (ABCD type spin system). The b-H and c-H signals of cyclobutane *rctt-3b* strongly overlap; therefore, the multiplicity of the signals of the four cyclobutane ring protons is more sophisticated, which makes it difficult to determine the spin-spin coupling constants.

Compounds *rctt-3b-d* were isolated by fractional crystallization in 33–70% yields and characterized by elemental analysis, ^1H and ^{13}C NMR spectroscopy (ESI, Figs. S8–S10 and S12–14), and UV–Vis spectrometry (ESI, Fig. S15). In the ^{13}C NMR spectra of *rctt-3b-d* (ESI, Figs. S12–S14), four signals corresponding to unsymmetrically substituted

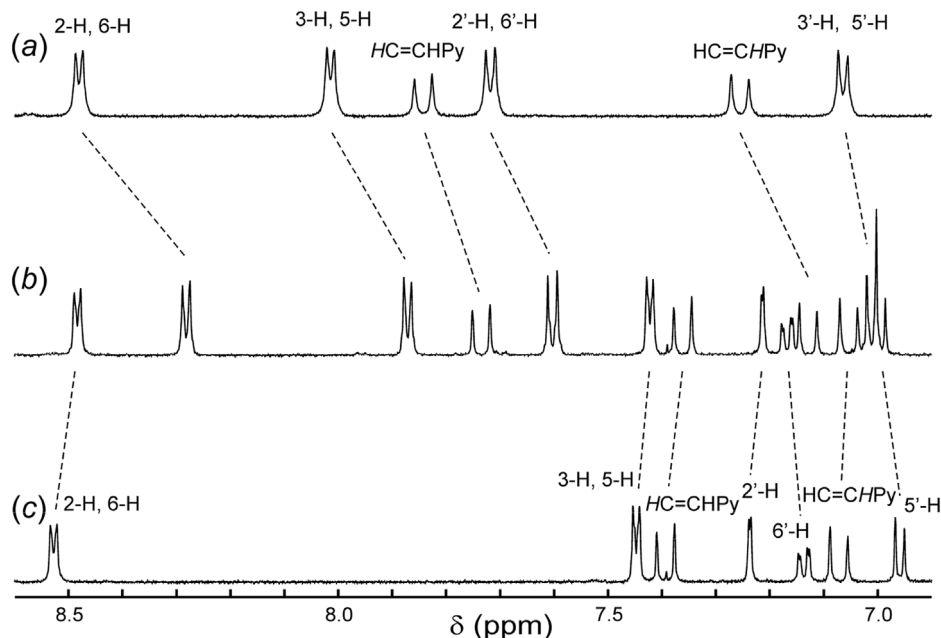


Fig. 3. ^1H NMR spectra (aromatic proton region) of (a) dye $(E)\text{-2b}$, (b) a 1:1 mixture of $(E)\text{-1b}$ and $(E)\text{-2b}$, and (c) compound $(E)\text{-1b}$; 1.1×10^{-3} M, $\text{MeCN-d}_3\text{-D}_2\text{O}$ (98:2, v/v), 30°C .

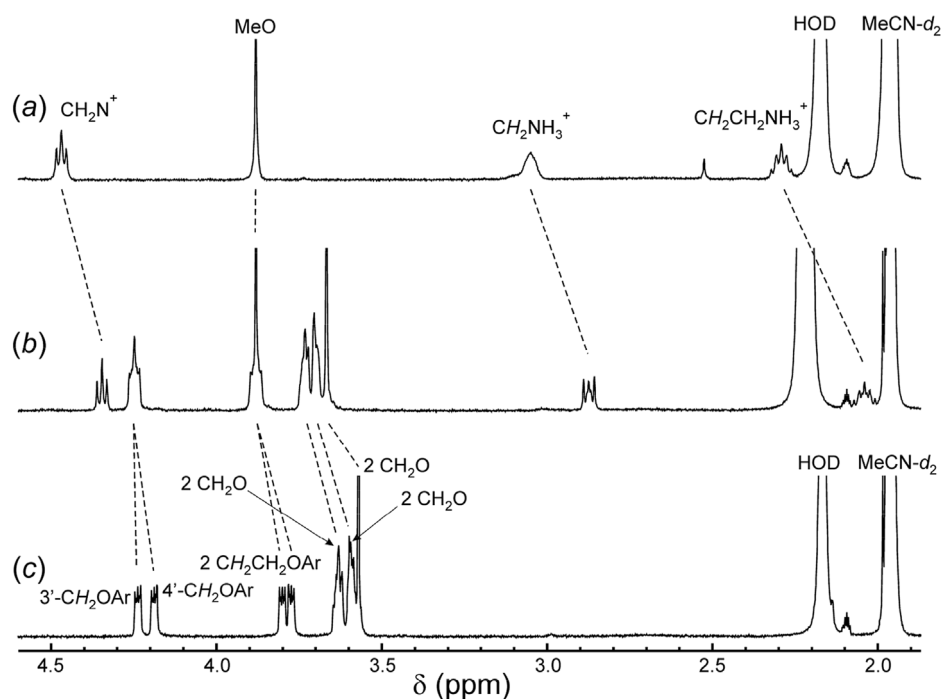


Fig. 4. ^1H NMR spectra (aliphatic proton region) of (a) dye (*E*)-**2b**, (b) a 1:1 mixture of (*E*)-**1b** and (*E*)-**2b**, and (c) compound (*E*)-**1b**; 1.1×10^{-3} M, $\text{MeCN-}d_3\text{-D}_2\text{O}$ (98:2, v/v), 30°C .

Table 3

Stability constants of the complexes of crown-compound (*E*)-**1b** with dyes (*E*)-**2a–g**.^a

complex	log <i>K</i>	complex	log <i>K</i>
(<i>E</i>)- 1b (<i>E</i>)- 2a	3.5 ^b	(<i>E</i>)- 1b (<i>E</i>)- 2e	3.5
(<i>E</i>)- 1b (<i>E</i>)- 2b	3.7	(<i>E</i>)- 1b (<i>E</i>)- 2f	3.6
(<i>E</i>)- 1b (<i>E</i>)- 2c	3.9	(<i>E</i>)- 1b (<i>E</i>)- 2g	3.5
(<i>E</i>)- 1b (<i>E</i>)- 2d	3.8		

^a ^1H NMR titration, $\text{MeCN-}d_3\text{-D}_2\text{O}$ (98:2, v/v), $30 \pm 1^\circ\text{C}$. The *K* values (M^{-1}) are measured to within about $\pm 30\%$.

^b From Ref. [19].

cyclobutane ring are present in the characteristic 42–48 ppm region. The ^{13}C signals of the cyclobutane ring of the previously studied compound *rctt*-**3a** are located in the same region (ESI, Fig. S11). The *rctt* stereochemistry for cyclobutanes **3b–d** was confirmed by X-ray diffraction analysis (Section 3.3).

Irradiation of an equimolar solution of compounds (*E*)-**1b** and (*E*)-**2g** also led to the formation of a cross-cycloadduct with *rctt* stereochemistry (according to ^1H NMR data). However, this photoproduct was insufficiently stable to be isolated in pure form (presumably, it isomerizes in the presence of basic impurities in the solvent [20]).

3.3. X-ray diffraction analysis

X-ray diffraction data for dyes (*E*)-**1a** [20], (*E*)-**2d** [38], (*E*)-**2f** [18], and (*E*)-**2g** [22] and cyclobutane *rctt*-**3a** [19] were reported previously. For crown-compound (*E*)-**1b**, single crystals suitable for X-ray diffraction analysis were obtained by co-crystallization with benzoic acid. The resulting structure is shown in Fig. 5.

The styrylpyridine moiety of molecule (*E*)-**1b** is slightly twisted, with the dihedral angle between the planes of the pyridine and benzene rings being 20.3° . The central double bond is substantially localized: the bond lengths in the $\text{C}(3)\text{--C}(6)=\text{C}(7)\text{--C}(8)$ moiety are 1.471(3), 1.336(4), and 1.464(3) Å. The macroheterocyclic moiety adopts a typical crown-like conformation preorganized to bind metal cations and

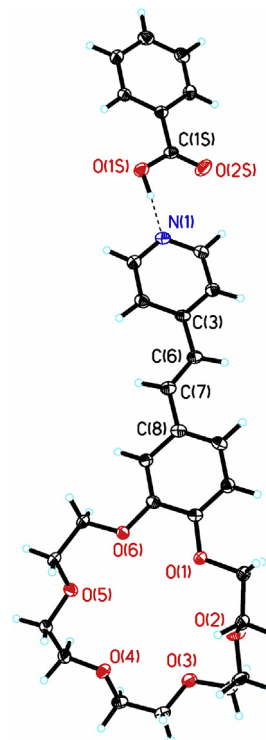


Fig. 5. Structure of (*E*)-**1b**PhCO₂H. Thermal ellipsoids are drawn at the 50% probability level. Hydrogen bond is drawn with a dashed line.

primary ammonium ions. The observed structural characteristics are typical of crystalline styrylheterocycles [18,20,22,38,39].

The benzoic acid molecule is nearly coplanar with the styrylpyridine moiety of (*E*)-**1b**; the dihedral angle between the benzene ring of benzoic acid and the pyridine ring of (*E*)-**1b** is only 10.9° . The PhCO₂H molecule forms a hydrogen bond with the pyridine nitrogen atom: the bond lengths in the $\text{O}(1\text{S})\text{--H}\cdots\text{N}(1)$ moiety are 1.01(3) and 1.60(3) Å,

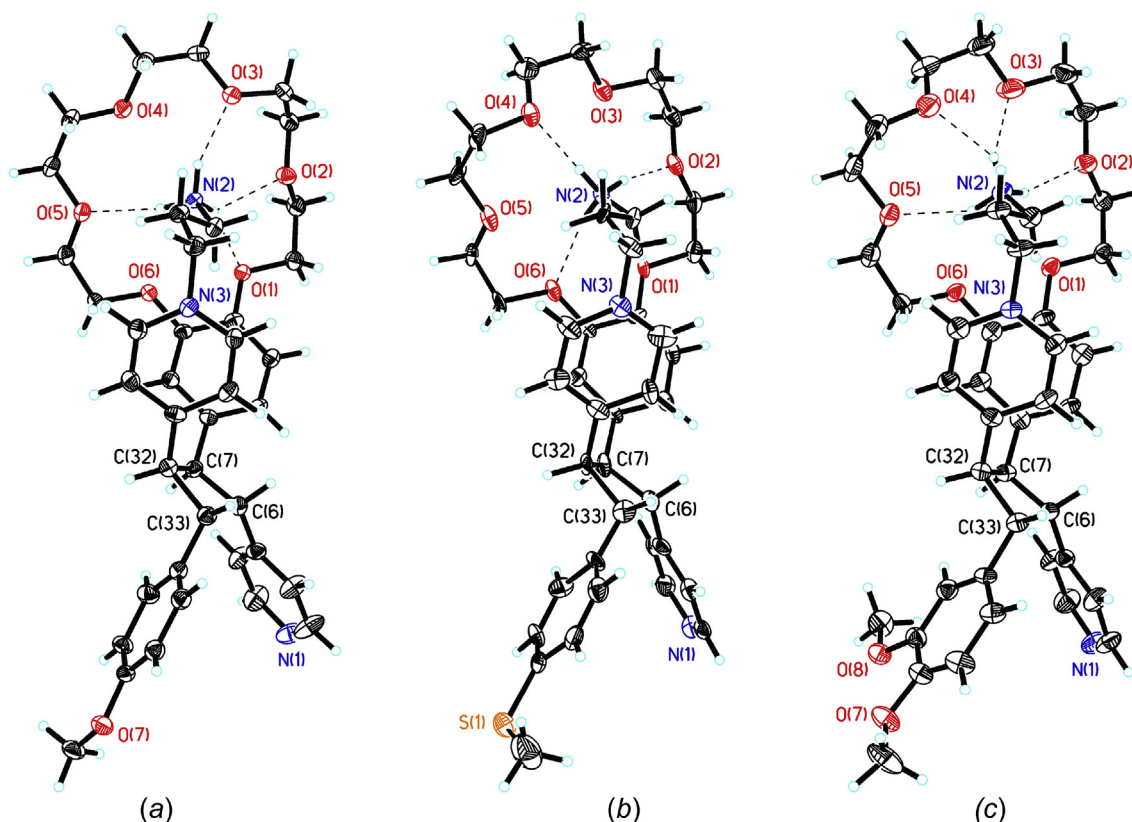


Fig. 6. Structure of the main components in (a) *rctt-3b*·C₆H₆, (b) *rctt-3c*·2C₆H₆·H₂O, and (c) *rctt-3d*·1.5C₆H₆. Thermal ellipsoids are drawn at the 30% probability level. Hydrogen bonds are drawn with dashed lines.

and the angle at the H atom is 177(3)°. Thus, the relatively weak organic acid does not protonate compound (*E*)-**1b**, and the acidic proton of the CO₂H group is not detached. Correspondingly, bond localization is observed in the O(2S)=C(1S)–O(1S) moiety: the bond lengths are 1.214(3) and 1.316(3) Å. The absence of protonation is indirectly confirmed by the fact that the crystals of (*E*)-**1b**·PhCO₂H are colorless, whereas the related dye (*E*)-**1a** and protonated form (*E*)-**1b**HClO₄, which contain positively charged pyridine residues, are bright yellow [20,39].

We were able to grow single crystals of cyclobutanes **3b–d** by slow saturation of their acetonitrile solutions with benzene vapor. The main components of the resulting structures are depicted in Fig. 6.

Although compounds **3b–d** crystallize in different space groups ($P2_1/n$ and $p\bar{1}$), they show similar geometric characteristics. All three cyclobutanes have *rctt* stereochemistry. The C(6)–C(7)–C(32)–C(33) cyclobutane rings are non-planar, the torsion angles in the rings vary between –13.2° and 13.0°, and the bond lengths are in the range of 1.521(7)–1.596(16) Å. All three structures are characterized by intramolecular hydrogen bonds (directional or bifurcated) between the ammonium group and the oxygen atoms of the 18-crown-6 ether moiety. The N(2)H...O bond lengths vary between 1.91 and 2.23 Å, and the angles at the H atoms do between 125° and 176°. Owing to the “tightening” effect of complexation, the C₅H₄N(3) pyridine ring comes closer to the benzene ring of the benzocrown ether moiety, unlike the other pair of *cis*-substituents, C₅H₄N(1) and C₆H₄O(S)Me [or C₆H₃(OMe)₂]. The dihedral angles for the former and latter pairs of *cis*-substituents in cyclobutanes **3b–d** vary between 38.2° and 41.4° and between 59.2° and 63.0°, respectively. Similar geometric characteristics have been observed for cyclobutane *rctt-3a* [19].

3.4. Molecular structure calculations

The molecular structures of crown-compound (*E*)-**1b**, dyes (*E*)-**2b,c**,

and complexes (*E*)-**1b**·(*E*)-**2b,c** in MeCN were studied by DFT/SMD calculations (computational details are given in Section 2.9). The Gibbs free energies in solution (G_{soln}) calculated for different conformers of (*E*)-**1b**, (*E*)-**2b,c**, and (*E*)-**1b**·(*E*)-**2b,c** are presented in Tables S1–S3 (ESI).

The lowest-energy conformers of (*E*)-**1b** and (*E*)-**2b** are shown in Fig. 7. The most stable conformation of (*E*)-**2c** is similar to that of (*E*)-**2b**.

Generally, compound (*E*)-**1b** can adopt two conformations, *s-trans* and *s-cis*, associated with rotation around the single bond between the olefinic bond and the benzocrown ether moiety. The difference in G_{soln}

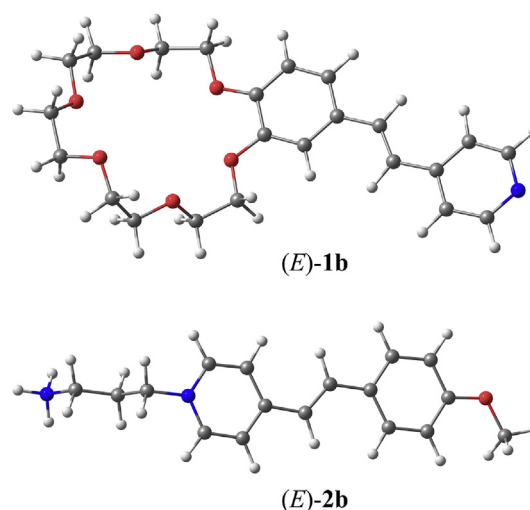


Fig. 7. Most stable conformers of crown-compound (*E*)-**1b** and dye (*E*)-**2b** in MeCN, according to DFT/SMD calculations.

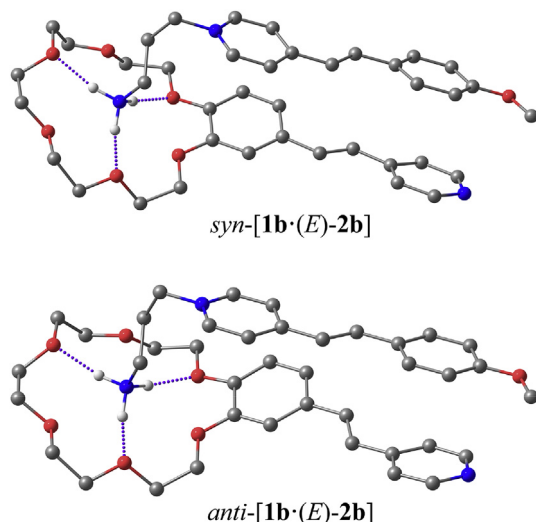


Fig. 8. Most stable conformations of *syn*- and *anti*-[1b(*E*)-2b] in MeCN, according to DFT/SMD calculations; hydrogen atoms are not shown except those of the ammonium group.

between the *s-trans* and *s-cis* conformers was calculated to be as low as $0.09 \text{ kcal mol}^{-1}$ in favor of the latter, which suggests the coexistence of these conformers in MeCN. The calculated bond lengths in the $\text{C}_{\text{Het}}-\text{C}=\text{C}-\text{C}_{\text{Ar}}$ bridge of (*s-cis*)-[*E*]-1b are 1.468, 1.344, and 1.466 Å, in good agreement with the corresponding bond lengths observed for the *s-trans* conformer of (*E*)-1b in crystals (Section 3.3); the deviations are as low as 0.1–0.6%.

In the most stable conformers of dyes (*E*)-2b,c, the ammoniopropyl substituent adopts all-*trans* conformation, and the OMe (SMe) group is in *s-cis* orientation with respect to the olefinic bond. The corresponding *s-trans* conformers are higher in energy by 0.34 and $0.17 \text{ kcal mol}^{-1}$ for (*E*)-2b and (*E*)-2c, respectively. For both dyes, the structures with *trans*, *gauche* conformation of the ammoniopropyl substituent are only slightly less stable than the lowest-energy conformers (the differences in G_{soln} do not exceed $0.5 \text{ kcal mol}^{-1}$).

Fig. 8 shows the lowest-energy conformations of complex 1b(*E*)-2b with the *syn* and *anti* orientations of the two olefinic bonds with respect to each other. The same conformations were found to be most stable for *syn*- and *anti*-[1b(*E*)-2c].

Both in the *syn* and *anti* structures, the ammoniopropyl substituent adopts *trans*, *gauche* conformation, and the styryl dye is in the *s-cis* conformation. Crown-compound (*E*)-1b adopts different conformations in the *syn* and *anti* structures (*s-trans* and *s-cis*, respectively).

The most stable *syn* conformers of 1b(*E*)-2b and 1b(*E*)-2c are lower in energy than the most stable *anti* conformers; in both cases, the difference in G_{soln} is approximately $0.7 \text{ kcal mol}^{-1}$. The distances between the centers of the two olefinic bonds in *syn*-[1b(*E*)-2b] and *syn*-[1b(*E*)-2c] are 3.53 and 3.49 Å, respectively, consistent with the topochemical criteria for PCA reactions [35,36]. The angle between these bonds is 23° in *syn*-[1b(*E*)-2b] and 24° in *syn*-[1b(*E*)-2c]. The fact that the olefinic bonds are nonparallel to each other may be one of the reasons for rather low quantum yields of the cross-PCA reaction in these complexes. In summary, the calculations predict that the differences in the topochemical parameters between the *syn* conformers of pseudodimers 1b(*E*)-2b and 1b(*E*)-2c are negligibly small and, in both cases, the *syn* conformers predominate over the *anti* conformers. This implies that the contrasting difference between these two pseudodimers in the cross-PCA rate constant (see discussion in Section 3.1) is due to electronic factors.

4. Conclusions

The absorption and fluorescence spectra, the emission lifetimes and quantum yields, and the *E-Z* photoisomerization quantum yields of *N*-(3-ammoniopropyl)-4-styrylpyridinium dyes (*E*)-2a–e vary dramatically depending on the nature and number of substituents (OMe, SMe, NMe₂) on the benzene ring. In the series of dyes (*E*)-2a–c (H, *p*-OMe, *p*-SMe), the barrier for *E-Z* photoisomerization increases with increasing the reorganization energy of the singlet excited state. Dye (*E*)-2e (*p*-NMe₂) is photoinert and virtually non-fluorescent, which is apparently attributable to fast transition from the initial excited state to the TICT state followed by nonradiative deactivation. For dye (*E*)-2d, which has two substituents on the benzene ring (*p*-OMe and *m*-OMe), there also exists a nonradiative deactivation pathway which is faster than the *E-Z* photoisomerization.

Styryl dyes (*E*)-2a–e and their analogs (*E*)-2f,g containing electron-withdrawing groups (NO₂, Cl) form, in MeCN, pseudodimeric complexes with the crown-containing styrylpyridine (*E*)-1b via hydrogen bonding between the ammonium group and the crown ether oxygen atoms. In these complexes, the styrylpyridinium and styrylpyridine moieties are located one above the other due to stacking interactions. The nature of substituents on the benzene ring of the styryl dye has little effect on the complex stability constant.

The formation of pseudodimeric complexes makes it possible to carry out [2 + 2]-cross-photocycloaddition of styryl dyes (*E*)-2a–d to styrylpyridine (*E*)-1b. The supramolecular reaction occurred stereospecifically to afford cyclobutanes 3a–d as single *rcct* isomers. The stereochemistry of cyclobutanes was confirmed by X-ray diffraction analysis. The cross-photocycloaddition quantum yields, measured upon selective excitation of the styryl dyes, and other relevant data suggested that the barrier for this photoreaction increases with an increase in the reorganization energy of the singlet excited state of the dye.

The results of this research can be used for the targeted design of photoactive supramolecular assemblies and in the development of new methods for the synthesis of cyclobutane derivatives using [2 + 2]-cross-photocycloaddition reactions.

Acknowledgements

This work was supported by the Russian Science Foundation with respect to the photochemical studies, the NMR studies, and the synthesis of cyclobutane derivatives [project No. 19-13-00020]; and by the Ministry of Science and Higher Education of the Russian Federation with respect to the DFT calculations [State Assignment No. 0089-2019-0003] and the synthesis of 4-styrylpyridine derivatives [State Assignment FSRC “Crystallography and Photonics” of RAS]. L.G.K. thanks the Royal Society of Chemistry for an International Author grant (with respect to the X-ray diffraction analysis). Authors thank Mr. Pavel S. Loginov for his help in synthesis and processing NMR titration experiments.

Appendix A. Supplementary data

Supplementary data to this article can be found online at <https://doi.org/10.1016/j.dyepig.2019.107825>.

References

- [1] Hoffmann N. Photochemical reactions as key steps in organic synthesis. *Chem Rev* 2008;108:1052–103. <https://doi.org/10.1021/cr0680336>.
- [2] Bach T, Hehn JP. Photochemical reactions as key steps in natural product synthesis. *Angew Chem Int Ed* 2011;50:1000–45. <https://doi.org/10.1002/anie.2011002845>.
- [3] Poplata S, Tröster A, Zou Y-Q, Bach T. Recent advances in the synthesis of cyclobutanes by olefin [2 + 2] photocycloaddition reactions. *Chem Rev* 2016;116:9748–815. <https://doi.org/10.1021/acs.chemrev.5b00723>.
- [4] Ushakov EN, Gromov SP. Supramolecular methods for controlling intermolecular [2 + 2] photocycloaddition reactions of unsaturated compounds in solutions. *Russ Chem Rev* 2015;84:787–802. <https://doi.org/10.1070/RCR4514>.

- [5] Ramamurthy V, Sivaguru J. Supramolecular photochemistry as a potential synthetic tool: Photocycloaddition. *Chem Rev* 2016;116:9914–93. <https://doi.org/10.1021/acs.chemrev.6b00040>.
- [6] Ushakov EN, Vedernikov AI, Lobova NA, Dmitrieva SN, Kuz'mina LG, Moiseeva AA, Howard JAK, Alfimov MV, Gromov SP. Supramolecular dimerization and [2 + 2] photocycloaddition reactions of crown ether styryl dyes containing a tethered ammonium group: structure–property relationships. *J Phys Chem A* 2015;119:13025–37. <https://doi.org/10.1021/acs.jpca.5b10758>.
- [7] Ushakov EN, Martyanov TP, Vedernikov AI, Pikalov OV, Efremova AA, Kuz'mina LG, Howard JAK, Alfimov MV, Gromov SP. Self-assembly through hydrogen bonding and photochemical properties of supramolecular complexes of bis(18-crown-6)stilbene with alkanediammonium ions. *J Photochem Photobiol A Chem* 2017;340:80–7. <https://doi.org/10.1016/j.jphotochem.2017.03.003>.
- [8] Berdnikova DV, Aliyev TM, Delbaere S, Fedorov YV, Jonusauskas G, Novikov VV, et al. Regio- and stereoselective [2 + 2] photocycloaddition in Ba²⁺ templated supramolecular dimers of styryl-derivatized aza-heterocycles. *Dyes Pigments* 2017;139:397–402. <https://doi.org/10.1016/j.dyepig.2016.11.053>.
- [9] Darcos V, Griffith K, Sallenave X, Desvergne J-P, Guyard-Duhayon C, Hasenknopf B, Bassani DM. Supramolecular control of [2 + 2] photodimerization via hydrogen bonding. *Photochem Photobiol Sci* 2003;2:1152–61. <https://doi.org/10.1039/B307525G>.
- [10] Skene WG, Couzigné E, Lehn J-M. Supramolecular control of the template-induced selective photodimerization of 4-methyl-7-O-hexylcoumarin. *Chem Eur J* 2003;9:5560–6. <https://doi.org/10.1002/chem.200305268>.
- [11] Gan M-M, Liu J-Q, Zhang L, Wang Y-Y, Hahn FE, Han Y-F. Preparation and post-assembly modification of metallosupramolecular assemblies from poly(*N*-heterocyclic carbene) ligands. *Chem Rev* 2018;118:9587–641. <https://doi.org/10.1021/acs.chemrev.8b00119>.
- [12] Ma L-L, An Y-Y, Sun L-Y, Wang Y-Y, Hahn FE, Han Y-F. Supramolecular control of photocycloadditions in solution: in situ stereoselective synthesis and release of cyclobutanes. *Angew Chem Int Ed* 2019;58:3986–91. <https://doi.org/10.1002/anie.201900221>.
- [13] Yamada S, Kusafuka M, Sugawara M. [2 + 2] Photodimerization of bispyridylethylenes by a controlled shift of the protonation equilibrium. *Tetrahedron Lett* 2013;54:3997–4000. <https://doi.org/10.1016/j.tetlet.2013.05.075>.
- [14] Yamada S, Nojiri Y. [2 + 2] Photodimerization of naphthylvinylpyridines through cation- π interactions in acidic solution. *Molecules* 2017;22:491. <https://doi.org/10.3390/molecules22030491>.
- [15] Sutyak KB, Lee W, Zavalij PV, Gutierrez O, Davis JT. Templating and catalyzing [2 + 2] photocycloaddition in solution using a dynamic G-quadruplex. *Angew Chem Int Ed* 2018;57:17146–50. <https://doi.org/10.1002/anie.201811202>.
- [16] Ushakov EN, Nadtochenko VA, Gromov SP, Vedernikov AI, Lobova NA, Alfimov MV, Gostev FE, Petrukhin AN, Sarkisov OM. Ultrafast excited state dynamics of the bi- and termolecular stilbene-viologen charge-transfer complexes assembled via host-guest interactions. *Chem Phys* 2004;298:251–61. <https://doi.org/10.1016/j.chemphys.2003.12.002>.
- [17] Ushakov EN, Martyanov TP, Vedernikov AI, Sazonov SK, Strelnikov IG, Klimenko LS, Alfimov MV, Gromov SP. Stereospecific [2 + 2]-cross-photocycloaddition in a supramolecular donor–acceptor complex. *Tetrahedron Lett* 2019;60:150–3. <https://doi.org/10.1016/j.tetlet.2018.11.077>.
- [18] Gromov SP, Vedernikov AI, Sazonov SK, Kuz'mina LG, Lobova NA, Strelenko YA, et al. Synthesis, structure, and stereospecific cross-[2 + 2] photocycloaddition of pseudodimeric complexes based on ammonioalkyl derivatives of styryl dyes. *New J Chem* 2016;40:7542–56. <https://doi.org/10.1039/c5nj03500g>.
- [19] Vedernikov AI, Sazonov SK, Kuz'mina LG, Howard JAK, Alfimov MV, Gromov SP. Stereospecific [2 + 2] photocycloaddition in a pseudodimeric complex between *N*-ammoniopropylstyrylpyridine and 18-crown-6-containing styrylpyridine. *Russ Chem Bull* 2009;58:1955–61. <https://doi.org/10.1007/s11172-009-0267-0>.
- [20] Vedernikov AI, Gromov SP, Lobova NA, Kuz'mina LG, Strelenko YA, Howard JAK, et al. Stereospecific solid-state [2 + 2] autophotocycloaddition of a styryl dye containing a 18-crown-6 fragment. *Russ Chem Bull* 2005;54:1954–66. <https://doi.org/10.1007/s11172-006-0064-y>.
- [21] Vedernikov AI, Lobova NA, Aleksandrova NA, Gromov SP. Study of complexation of styrylheterocycles with cavitands by spectroscopic methods. *Russ Chem Bull* 2015;64:2459–72. <https://doi.org/10.1007/s11172-015-1178-x>.
- [22] Ushakov EN, Vedernikov AI, Sazonov SK, Kuz'mina LG, Alfimov MV, Howard JAK, Gromov SP. Synthesis and photochemical study of a supramolecular pseudodimeric complex of 4-styrylpyridinium derivatives. *Russ Chem Bull* 2015;64:562–72. <https://doi.org/10.1007/s11172-015-0901-y>.
- [23] Vedernikov AI, Sazonov SK, Loginov PS, Lobova NA, Alfimov MV, Gromov SP. Hydrogen bonding- and stacking-induced stereospecific [2 + 2]-photocycloaddition within a pseudodimeric complex of two styryl dyes. *Mendeleev Commun* 2007;17:29–31. <https://doi.org/10.1016/j.mencom.2007.01.012>.
- [24] Suzuki K, Kobayashi A, Kaneko S, Takehira K, Yoshihara T, Ishida H, Shiina Y, Oishi S, Tobita S. Reevaluation of absolute luminescence quantum yields of standard solutions using a spectrometer with an integrating sphere and a back-thinned CCD detector. *Phys Chem Chem Phys* 2009;11:9850–60. <https://doi.org/10.1039/B912178A>.
- [25] Frassinetti C, Ghelli S, Gans P, Sabatini A, Moruzzi MS, Vacca A. Nuclear magnetic resonance as a tool for determining protonation constants of natural polyprotic bases in solution. *Anal Biochem* 1995;231:374–82. <https://doi.org/10.1006/abio.1995.9984>.
- [26] Sheldrick GM. Crystal structure refinement with SHELXL. *Acta Crystallogr C* 2015;71:3–8. <https://doi.org/10.1107/S2053229614024218>.
- [27] Gaussian 16, revision A.03. Wallingford CT: Gaussian, Inc.; 2016.
- [28] Zhao Y, Truhlar DG. The M06 suite of density functionals for main group thermochemistry, thermochemical kinetics, noncovalent interactions, excited states, and transition elements: two new functionals and systematic testing of four M06-class functionals and 12 other functionals. *Theor Chem Acc* 2008;120:215–41. <https://doi.org/10.1007/s00214-007-0310-x>.
- [29] Marenich AV, Cramer CJ, Truhlar DG. Universal solvation model based on solute electron density and on a continuum model of the solvent defined by the bulk dielectric constant and atomic surface tensions. *J Phys Chem B* 2009;113:6378–96. <https://doi.org/10.1021/jp810292n>.
- [30] Strehmel B, Seifert H, Rettig W. Photophysical properties of fluorescence probes. 2. A model of multiple fluorescence for stilbazolium dyes studied by global analysis and quantum chemical calculations. *J Phys Chem B* 1997;101:2232–43. <https://doi.org/10.1021/jp962835v>.
- [31] Cao X, Tolbert RW, McHale JL, Edwards WD. Theoretical study of solvent effects on the intramolecular charge transfer of a hemicyanine dye. *J Phys Chem A* 1998;102:2739–48. <https://doi.org/10.1021/jp972190e>.
- [32] Löhr H-G, Vögtle F. Chromo- and fluoroionophores. A new class of dye reagents. *Acc Chem Res* 1985;18:65–72. <https://doi.org/10.1021/ar00111a001>.
- [33] Tsukanov AV, Dubonosov AD, Bren VA, Minkin VI. Organic chemosensors with crown-ether groups. *Chem Heterocycl Comp* 2008;44:899–923. <https://doi.org/10.1007/s10593-008-0132-3>.
- [34] Jordanides XJ, Lang MJ, Song X, Fleming GR. Solvation dynamics in protein environments studied by photon echo spectroscopy. *J Phys Chem B* 1999;103:7995–8005. <https://doi.org/10.1021/jp9910993>.
- [35] Schmidt GMJ. Photodimerization in the solid state. *Pure Appl Chem* 1971;27:647–78. <https://doi.org/10.1351/pac197127040647>.
- [36] Ramamurthy V, Venkatesan K. Photochemical reactions of organic crystals. *Chem Rev* 1987;87:433–81. <https://doi.org/10.1021/cr00078a009>.
- [37] Vedernikov AI, Ushakov EN, Lobova NA, Kiselev AA, Alfimov MV, Gromov SP. Photosensitive molecular tweezers. 3. Synthesis and homoditopic complex formation of a bisstyryl dye containing two crown-ether fragments with diammonium ions. *Russ Chem Bull* 2005;54:666–72. <https://doi.org/10.1007/s11172-005-0303-7>.
- [38] Gromov SP, Vedernikov AI, Kuz'mina LG, Kondratuk DV, Sazonov SK, Strelenko YA, et al. Photocontrolled molecular assembler based on cucurbit[8]uril: [2 + 2]-autophotocycloaddition of styryl dyes in the solid state and in water. *Eur J Org Chem* 2010:2587–99. <https://doi.org/10.1002/ejoc.200901324>.
- [39] Kuz'mina LG, Vedernikov AI, Sazonov SK, Lobova NA, Churakov AV, Lermontova EK, Howard JAK, Alfimov MV, Gromov SP. Design of crystal packings of styrylheterocycles and [2 + 2] photocycloaddition reactions in their single crystals. 7. Crystal structures of 4-styrylpyridine hydroperchlorates and solid-state [2 + 2] autophotocycloaddition reactions of these compounds. *Russ Chem Bull* 2011;60:1734–61. <https://doi.org/10.1007/s11172-011-0259-8>.